

term hypersensitization to repeated stimuli shown by cholinergic brain tracts may be due to this substitution.

References and Notes

- B. S. McEwen, *Annu. Rev. Neurosci.* **22**, 105 (1999).
- R. M. Sapolsky, L. M. Romero, A. U. Munck, *Endocr. Rev.* **21**, 55 (2000).
- G. Mezey, I. Robbins, *Brit. Med. J.* **323**, 56 (2001).
- J. A. McCormick et al., *Mol. Endocrinol.* **14**, 506 (2000).
- J. Xie, D. P. McCobb, *Science* **280**, 443 (1998).
- R. Daoud, M. Da Penha Berzaghi, F. Siedler, M. Hubener, S. Stamm, *Eur. J. Neurosci.* **11**, 788 (1999).
- L. Davis, G. A. Banker, O. Steward, *Nature* **330**, 477 (1987).
- J. A. Foster, I. R. Brown, *J. Neurosci. Res.* **46**, 652 (1996).
- O. Steward, C. S. Wallace, G. L. Lyford, P. F. Worley, *Neuron* **21**, 741 (1998).
- H. Kang, E. M. Schuman, *Science* **273**, 1402 (1996).
- C. H. Bailey, D. Bartsch, E. R. Kandel, *Proc. Natl. Acad. Sci. U.S.A.* **93**, 13445 (1996).
- O. Steward, E. M. Schuman, *Annu. Rev. Neurosci.* **24**, 299 (2001).
- H. Soreq, S. Seidman, *Nature Rev. Neurosci.* **2**, 294 (2001).
- Poly-L-ornithine-coated cover slips [0.5 mg ml⁻¹, 10 min at room temperature (RT)] were sterilized by ultraviolet irradiation (TUV/c 8 W, 3 hours at RT). Cover slip-grown cells were fixed in 3% paraformaldehyde (20 min), dried (1 hour at 37°C), washed 2 × 5 min in phosphate-buffered saline (PBS) and 2 × 5 min in 0.2% Tween-20 PBS (PBT), incubated with 10 mg/ml proteinase K (5 min at RT), and rewashed (PBT, 2 × 5 min). Streptavidin (1 mg ml⁻¹, 30 min at RT) served to block nonspecific labeling. Hybridization was in a humidified chamber with 10 μg ml⁻¹ probe in 50% formamide, 5 × SSC, 10 mg ml⁻¹ tRNA, 10 mg ml⁻¹ heparin (90 min at 52°C). Washes were in 50% formamide, 5 × SSC, and 0.5% sodium dodecyl sulfate, and in 50% formamide, 2 × SSC at 60°C, then at RT in tris-buffered saline (pH 7.5), with 0.1% Tween-20 (TBST) including 2 mM levamisole. Following blockade in 1% skim milk (30 min), digoxigenin-labeled probes were detected with fluorescein- or rhodamine-labeled anti-DIG antibodies (1 hour at RT, three washes in TBST). Biotin-labeled probes were detected (a) fluorometrically by conjugation with streptavidin-Cy2 or -Cy3 (Figs. 1 and 2) or (b) the ELF method (Molecular Probes, Eugene, OR) (Fig. 4, E and F), or (c) colorimetrically with streptavidin-alkaline phosphatase conjugates using Fast Red (Roche Diagnostics, Mannheim, Germany) (Fig. 3, E to J, and Fig. 4, A to D). Mounting was with Immu-Mount (Shandon, Pittsburgh, PA).
- N. Galyam et al., *Antisense Nucleic Acid Drug Dev.* **11**, 51 (2001).
- M. Schramm, S. Eimerl, E. Costa, *Proc. Natl. Acad. Sci. U.S.A.* **87**, 1193 (1990).
- D. Kaufer, A. Friedman, S. Seidman, H. Soreq, *Nature* **393**, 373 (1998).
- Following hybridization with an AChE-R cRNA probe, 43 of 50 PC12 cells and 45 of 50 cultured primary cerebellar neurons displayed nuclear as well as cytoplasmic labeling. In contrast, only 9 of 50 PC12 cells and 5 of 50 primary neurons labeled for AChE-S mRNA showed nuclear labeling, reflecting different ratios of nuclear pre-mRNA to mature variant transcripts.
- H. Soreq, D. Zevin-Sonkin, N. Razon, *EMBO J.* **3**, 1371 (1984).
- M. Shapira et al., *Hum. Mol. Genet.* **9**, 1273 (2000).
- When treated with 1.5 nM INV101, an oligonucleotide of sequence inverse to EN101, both PC12 cells and cultured primary cerebellar neurons were labeled as extensively as untreated cells with both AChE-S and AChE-R cRNAs ($n = 20$ cells; SD < 17 and 12%, respectively, and $P > 0.5$ for the two probes).
- Supplementary material is available at www.sciencemag.org/cgi/content/full/295/5554/508/DC1
- Samples were incubated with monoclonal anti-AChE-S antibodies (Transduction Laboratories, San Diego, CA), dilution 1:200, 1 hour at RT overnight 4°C, then similar incubations with HRP-tagged goat anti-mouse secondary antibodies (1:500). Detection was with Tyramide Signal Amplification system and Cy5 fluorophore (NEN Life Science Products, Boston, MA).
- C. Erb et al., *J. Neurochem.* **77**, 638 (2001).
- L. Davis, B. Burger, G. A. Banker, O. Steward, *J. Neurosci.* **10**, 3056 (1990).
- C. S. Wallace, G. L. Lyford, P. F. Worley, O. Steward, *J. Neurosci.* **18**, 26 (1998).
- R. Gray, A. S. Rajan, K. A. Radcliffe, M. Yakehiro, J. A. Dani, *Nature* **383**, 713 (1996).
- A. Friedman, D. Kaufer, L. Pavlovsky, H. Soreq, *J. Physiol. Paris* **92**, 329 (1998).
- S. M. Antelman, A. J. Eichler, C. A. Black, D. Kocan, *Science* **207**, 329 (1980).
- A. Blichenberg et al., *J. Neurosci.* **19**, 8818 (1999).
- R. Y. Chan, F. A. Adatia, A. M. Krupa, B. J. Jasmin, *J. Biol. Chem.* **273**, 9727 (1998).
- J. Guhaniyogi, G. Brewer, *Gene* **265**, 11 (2001).
- Z. D. Luo et al., *Mol. Pharmacol.* **56**, 886 (1999).
- T. G. Aigner, *Curr. Opin. Neurobiol.* **5**, 155 (1995).
- A. Imperato, S. Puglisi-Allegra, P. Casolini, L. Angelucci, *Brain Res.* **538**, 111 (1991).
- We thank K. Löffleholz and J. Klein (Mainz) for fruitful discussions and N. Melamed-Book (Jerusalem) for assistance. Supported by the U.S. Army Medical Research and Materiel Command (DAMD 17-99-1-9547 to H.S. and A.F.), U.S.-Israel Binational Science Foundation (1999/115 to H.S., 1998/066 to N.B.-A., 1997/00174 to A.F.), European Community (QLG3-CT-2000-00072 to N.B.-A.), and Ester Neuroscience, Ltd. (to H.S.). C.E. was a Minerva Foundation postdoctoral fellow.

2 October 2001; accepted 30 November 2001

Dynamics and Constancy in Cortical Spatiotemporal Patterns of Orientation Processing

Dahlia Sharon* and Amiram Grinvald

How does the high selectivity to stimulus orientation emerge in the visual cortex? Thalamic feedforward-dominated models of orientation selectivity predict constant selectivity during the visual response, whereas intracortical recurrent models predict dynamic improvement in selectivity. We imaged the cat visual cortex with voltage-sensitive dyes to measure orientation-tuning dynamics of a large neuronal population. Tuning-curve width did not narrow after response onset, whereas the difference between preferred and orthogonal responses (modulation depth) first increased, then declined. We identified a suppression of the evoked responses, referred to as the evoked deceleration-acceleration (DA) notch, which was larger for the orthogonal response. Furthermore, peak selectivity of the tuning curves was contemporaneous with the evoked DA notch. These findings suggest that in the cat brain, sustained visual cortical processing does not narrow orientation tuning; rather, intracortical interactions may amplify modulation depth and suppress the orthogonal response relatively more than the preferred. Thus, feedforward models and recurrent models of orientation selectivity must be combined.

Visual cortical neurons are highly selective for the orientation of stimuli presented within their receptive field (1), a property not shared by their thalamic inputs (2). How orientation selectivity arises in the cortex is still debated. Previous experiments (3–10) have suggested mechanisms that include feedforward (thalamically dominated) (1, 11) and recurrent (intracortically dominated) (12–15) models. The input impinging on orientation-selective neurons has constant selectivity in feedforward models, whereas recurrent models predict improvement in selectivity during the visual response. Although single-unit methodologies excel at determining the properties of individual neurons, these properties are

highly variable, making it extraordinarily difficult to obtain large samples on which to base estimates of neuronal population behavior. In optical imaging with voltage-sensitive dyes (16), the recorded signal accurately represents membrane-potential changes at the neuronal population level (17, 18), emphasizing synaptic potentials in the dendritic tufts of cortical neurons from superficial and deep layers. Recently, this method has been improved substantially, enabling in vivo imaging of cortical neuronal population activity with millisecond temporal resolution and spatial resolution of 50 to 100 μm (19). We therefore used optical imaging to explore the dynamics of orientation selectivity (9, 20–22).

We imaged the responses of area 18 in the cat visual cortex to high-contrast square-wave gratings of six different orientations (23). We examined the recording period starting 50 ms before stimulus onset and lasting 300 ms (thus avoiding late intrinsic signal

Department of Neurobiology and the Center for Studies of Higher Brain Functions, Weizmann Institute of Science, Rehovot 76100, Israel.

*To whom correspondence should be addressed. E-mail: dahlia.sharon@weizmann.ac.il

REPORTS

artifacts). Figure 1A shows the evoked response (24) to 150° gratings at a sampling rate of 9.6 ms per frame: the time series of single-condition responses (25), normalized to activity recorded during presentation of a blank screen. At 36 ms after stimulus onset, a brightening began (the dye fluorescence increased in response to depolarization) across the entire imaged area rather than only in the preferred orientation patches. Thus, this brightening signal had both an orientation-nonselective component and an orientation-selective component (Fig. 1, A and B).

We examined the orientation-selective response by fitting a Gaussian to the tuning curve (26) at every point in time (27), as exemplified in Fig. 1C for the data frame at 65 ms, for pixels within the delineated re-

gions of Fig. 1A (rightmost frame). Preferred orientation is obtained from the peak angle of the Gaussian. Selectivity is determined by three additional independent attributes of the tuning curve, obtained from the Gaussian fit (27): half width at half height (HWHH), modulation depth (MD, preferred – orthogonal), and nonselective component (NSC). We combined these attributes into a single selectivity index (28).

We analyzed preferred orientation, obtained from pixel-by-pixel Gaussian fitting (26, 27) from the same hemisphere shown in Fig. 1. Figure 2A shows a sequence of polar maps (29) in which preferred orientation and MD are represented by color and brightness, respectively. After the map emerged at 36 ms, its strength increased until 74 ms. Before

one can draw any conclusions from these maps, it is important first to examine their reproducibility by comparing two independent subsets of stimulus presentations. Before response onset, the apparent “orientation map” was not reproducible, whereas it reached near-maximal reproducibility at 46 ms, ~10 ms after response onset (18). All subsequent analysis was done exclusively for the pixels in the high-reproducibility region indicated by the dotted line (in Fig. 2C).

Qualitative visual inspection of Fig. 2A suggested that preferred orientation at each cortical location was stable over time, because the color at each pixel did not change appreciably between frames in the time sequence. This was quantified by comparing the map at each frame to a high signal-to-noise ratio map. Figure 2B demonstrates the correlation coefficient between preferred orientation in each frame and in this average map (Fig. 2C). As soon as the response was fully reproducible (46 ms, close to the time of the first cortical spikes) (18), the correlation coefficient stabilized at ~0.8, and the change in preferred orientation between successive frames had a median of 4.4°, well within the effect of residual noise in the images. Having observed the same result in two additional hemispheres, we concluded that as soon as the signal was reproducible, preferred orientation was constant as a function of time.

We next calculated the evolution in time of orientation selectivity for the entire population by Gaussian fitting of the tuning curve averaged over all pixels delineated in Fig. 2C, on a frame-by-frame basis. Figure 3A shows the tuning curves and their fits for a few frames for the same hemisphere shown in Figs. 1 and 2. To facilitate comparison, we removed the offset of the tuning curves (NSC) so that they all started at the same baseline value of 0. These tuning curves suggest that as the response develops, MD increases, but tuning width does not change

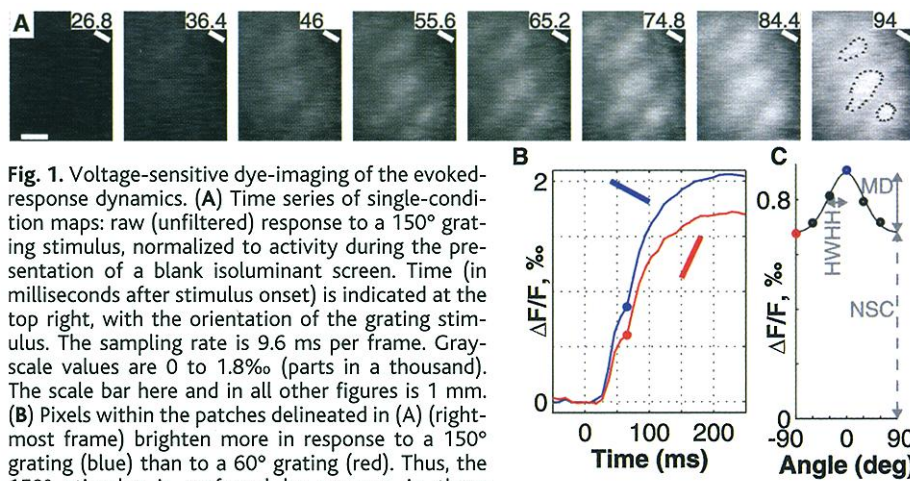


Fig. 1. Voltage-sensitive dye-imaging of the evoked-response dynamics. (A) Time series of single-condition maps: raw (unfiltered) response to a 150° grating stimulus, normalized to activity during the presentation of a blank isoluminant screen. Time (in milliseconds after stimulus onset) is indicated at the top right, with the orientation of the grating stimulus. The sampling rate is 9.6 ms per frame. Gray-scale values are 0 to 1.8% (parts in a thousand). The scale bar here and in all other figures is 1 mm. (B) Pixels within the patches delineated in (A) (rightmost frame) brighten more in response to a 150° grating (blue) than to a 60° grating (red). Thus, the 150° stimulus is preferred by neurons in these patches. The y axis is the fractional response ($\Delta F/F$, %) (the brightness of pixels relative to the resting fluorescence level). The two dots highlight the evoked DA notch (see text). (C) Orientation tuning curve, for the pixels delineated in (A) (rightmost frame), at the time marked by the two dots in (B), with the best-fitting Gaussian. HWHH, MD, and NSC are marked by arrows. The NSC here is considerably larger than that normally reported in simple cells. However, the optical signal is dominated by the superficial layers, in which the more common neurons are complex cells. In these cells, the intracellular NSC is considerably larger than in simple cells—in a few cells it was up to 67%, although in others it was almost absent (39). Furthermore, the optical signal emphasizes activity in dendritic tufts that spread laterally, beyond the borders of orientation domains of neuronal somata.

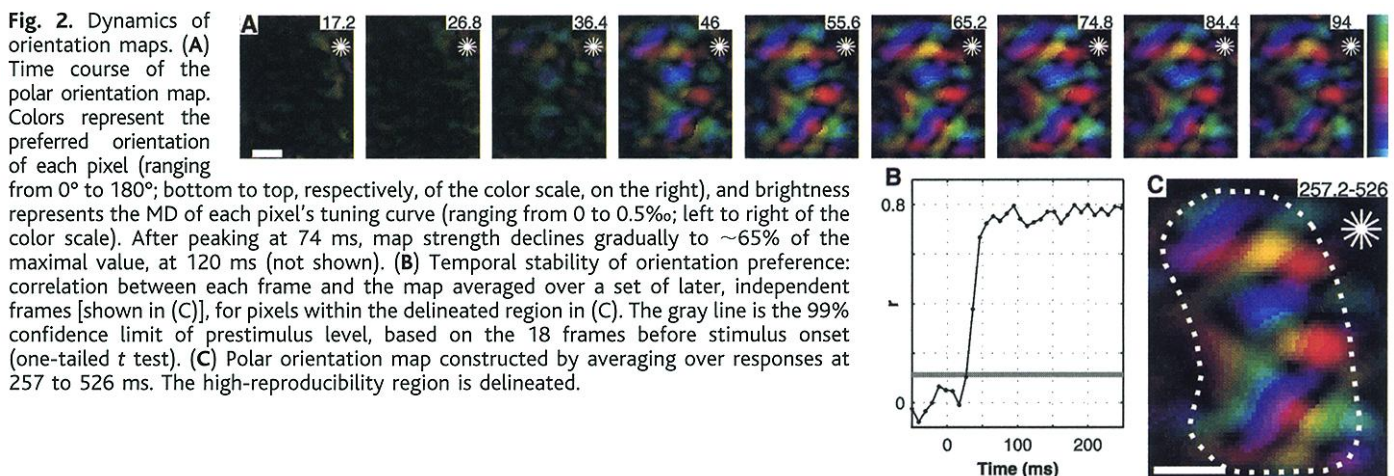


Fig. 2. Dynamics of orientation maps. (A) Time course of the polar orientation map. Colors represent the preferred orientation of each pixel (ranging from 0° to 180°; bottom to top, respectively, of the color scale, on the right), and brightness represents the MD of each pixel’s tuning curve (ranging from 0 to 0.5%; left to right of the color scale). After peaking at 74 ms, map strength declines gradually to ~65% of the maximal value, at 120 ms (not shown). (B) Temporal stability of orientation preference: correlation between each frame and the map averaged over a set of later, independent frames [shown in (C)], for pixels within the delineated region in (C). The gray line is the 99% confidence limit of prestimulus level, based on the 18 frames before stimulus onset (one-tailed *t* test). (C) Polar orientation map constructed by averaging over responses at 257 to 526 ms. The high-reproducibility region is delineated.

REPORTS

appreciably. We used two different approaches to assess the reliability of the Gaussian fits and the parameters derived from them (18). The response for early data points was small and indistinguishable from background noise (marked in red and orange). The first frames that showed highly reliable fits are marked in green throughout Fig. 3. For the three experiments shown in Fig. 3, a reliable fit was obtained already in the first or second frame after onset of the evoked responses (e.g., Fig. 1B).

Figure 3B shows the time course of orientation tuning width. HWHH of the fitted Gaussian started at 35.5° already in the first frame with an acceptable fit, at 36 ms. It then widened gradually to ~38° during about the next 60 ms. For the three experiments, the narrowest initial values of HWHH range from 33° to 36°, and late values range from 36° to 38°. This range is well within that found for the intracellular response averaged over hundreds of milliseconds (30–33). Therefore, the measurement of tuning dynamics averaged over several populations of thousands of neu-

rons did not show an improvement in tuning width (narrowing) as cortical response continued to increase (Fig. 1B).

Modulation depth is presented in Fig. 3C as the amplitude of the fitted Gaussian. It increased until 74 ms after stimulus onset (during the first 50 ms of the response), after which it decreased to a relatively stable level of ~65% of maximal response during the course of ~40 ms. This behavior was consistent in all three hemispheres, with a late MD of 65 to 90% of the peak value. Moreover, because MD is the difference between preferred and orthogonal responses, it can be assessed in experiments in which only two orientations were presented, and these results were confirmed in the other 10 hemispheres in this study (18), in which only two stimulus orientations were used. Taken together, we concluded that MD peaked tens of milliseconds after cortical response began, rather than at its onset.

To evaluate overall selectivity, we determined the selectivity index (Fig. 3D) (28). After response onset, selectivity increased and peaked at 55 ms, decaying to about one-

third of its peak value at ~150 ms. Because HWHH is fairly constant throughout the response (Fig. 3B), this temporal profile was affected mainly by the ratio between the selective component (MD) and the nonselective one. This normalized MD (preferred – orthogonal/orthogonal) peaked at 55 to 100 ms over the additional 10 hemispheres in this study (18).

What mechanisms are involved in creating the peak in selectivity observed 55 to 100 ms after response onset? One possibility is suggested by the finding that the selectivity index (as well as normalized MD) peaked simultaneously with a small transient drop in the rate at which the evoked response increased. This deceleration and subsequent acceleration, which we term the evoked deceleration-acceleration (DA) notch, is marked by two dots in Fig. 1B and suggests a temporary suppression: The response first slowed down, then sped up. Peak selectivity (Fig. 3D) was attained at the same time, at 55 ms. The evoked DA notch was detected in 12 of the 13 hemispheres examined. Because the evoked DA notch is rather small, we investigated whether it was present in existing in vivo intracellular recordings in area 18 of the cat visual cortex (34). Not surprisingly, we detected the notch in the averaged intracellular recording of the visually evoked response.

Enlargements of two optically detected evoked DA notches are shown in the red and green insets of Fig. 4 [for the complete set of

Fig. 3. Dynamics of orientation selectivity. (A) Tuning curves (mean ± SE) were averaged over pixels in the reproducible region (Fig. 2C) for several frames, the times of which are indicated on the right. The hemisphere used was the same as that in Figs. 1 and 2. (Insets). Two additional experiments: the frames shown are the same as those in the main panel, with modifications of frame color notation shown in the small boxes. The blue- and magenta-colored insets in (A) to (D) show the same two experiments. Frame color notations are constant for each experiment; red and orange curves mark the last frames before reliable fits were obtained, and green curves mark the first frames with reliable fits. For the two experiments shown in the insets, the first frame of the response showed an intermediate significance level, marked in yellow (18). (B) Half-width at half-height (HWHH) obtained from a Gaussian fit. Ninety-nine percent confidence intervals (40) are shown in light and dark gray shading, for frames with reliable and unreliable fits, respectively; after response onset they were between 8° and 15° wide. (C) Amplitude (MD) of the Gaussian fit. Ninety-nine percent confidence intervals are shown in gray. (D) Selectivity index (28). We found that MD normalized by orthogonal, preferred, or [orthogonal + preferred] (33), as well as 1/[circular variance] (15), all exhibit an extremely similar time course to the selectivity index (not shown).

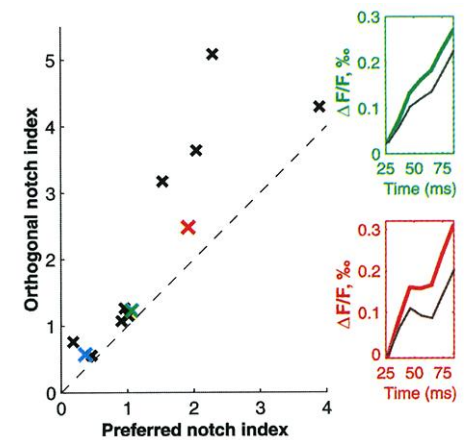
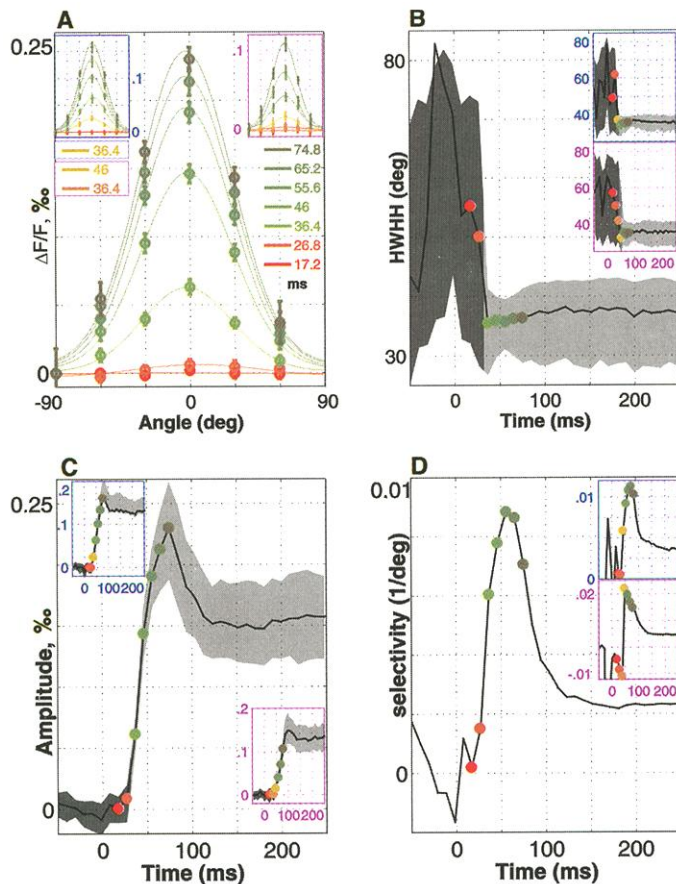


Fig. 4. The evoked DA notch. The orthogonal notch index (35) is larger than the preferred notch index for all 12 hemispheres. The green cross is from the experiment shown in Figs. 1 through 3 (main panels); the blue cross is from the experiment shown in the blue insets in Fig. 3. (Insets): The evoked response around notch occurrence. Green inset, as described above; red inset, an additional experiment (also shown in the main panel). The thick trace represents the response to preferred orientation, and the thin trace the response to orthogonal orientation. See also (18).

hemispheres, see (18)]. In these 12 hemispheres, peak normalized MD (or peak selectivity index, in the two hemispheres where six orientations were presented) occurred within 10 ms of the acceleration at the end of the evoked DA notch, with a correlation coefficient between the two events of 0.83 ($P < 0.001$, two-tailed t test). A comparison between the evoked DA notch at the preferred and orthogonal orientations (Fig. 4, insets) (18) showed that, although the magnitude of the evoked DA notch varied among experiments, it was always stronger for the orthogonal orientation than for the preferred. Comparison of the evoked DA notch index (35) at the orthogonal and preferred orientations is shown in Fig. 4 for the 12 hemispheres in which an evoked DA notch was detected. A larger notch index corresponds to a greater deflection of the response. Equal values lie on the dashed line, so in all cases the orthogonal stimulus induced a larger evoked DA notch than the preferred stimulus ($P < 0.01$, one-tailed paired t test). Therefore, analysis of the evoked DA notch suggests that suppression, which has a stronger relative influence when the orthogonal orientation is presented, coincides with maximal selectivity.

The data presented here imply that sustained cortical processing does not narrow tuning width and is not required to establish preferred orientation at a given cortical location (36). However, the dynamic time course of MD suggests that cortical interactions are involved in determining the amplification of the tuning curve; both intracortical excitation (12–14) and inhibition (7–11, 15, 37) may be involved. We identified an evoked DA notch in the evoked response at ~50 to 80 ms, which we interpret as the peaking of a suppressive mechanism, simultaneous with peak normalized (MD). Questions remain regarding the orientation selectivity of the underlying synaptic mechanism and whether it results from increased inhibition or from withdrawal of excitation. Shunting inhibition has been shown to peak as early as 50 to 70 ms (38), and in light of evidence for the involvement of cross-orientation inhibition in orientation selectivity (7, 10), we favor the involvement of inhibition. However, the present results suggest that the inhibition observed in these previous studies should be involved in amplifying rather than narrowing the tuning curve—increasing its normalized MD by preventing the response to the orthogonal orientation from increasing as rapidly as the response to the preferred orientation.

References and Notes

- D. H. Hubel, T. N. Wiesel, *J. Physiol. (London)* **160**, 106 (1962).
- _____, *J. Physiol. (London)* **155**, 385 (1961).
- D. Ferster, *J. Neurosci.* **6**, 1284 (1986).
- B. Chapman, K. R. Zahs, M. P. Stryker, *J. Neurosci.* **11**, 1347 (1991).
- R. C. Reid, J.-M. Alonso, *Nature* **378**, 281 (1995).
- D. Ferster, S. Chung, H. Wheat, *Nature* **380**, 249 (1996).
- A. M. Sillito, *J. Physiol. (London)* **250**, 305 (1975).
- A. B. Bonds, *Vis. Neurosci.* **2**, 41 (1989).
- D. L. Ringach, M. J. Hawken, R. Shapley, *Nature* **387**, 281 (1997).
- J. M. Crook, Z. F. Kisvarday, U. T. Eysel, *Vis. Neurosci.* **14**, 141 (1997).
- T. W. Troyer, A. E. Krukowski, N. J. Priebe, K. D. Miller, *J. Neurosci.* **18**, 5908 (1998).
- R. Ben-Yishai, R. L. Bar-Or, H. Sompolinsky, *Proc. Natl. Acad. Sci. U.S.A.* **92**, 3844 (1995).
- R. J. Douglas, C. Koch, M. Mahowald, K. A. C. Martin, H. H. Suarez, *Science* **269**, 981 (1995).
- D. C. Somers, S. B. Nelson, M. Sur, *J. Neurosci.* **15**, 5448 (1995).
- D. McLaughlin, R. Shapley, M. J. Shelley, D. J. Wiesel, *Proc. Natl. Acad. Sci. U.S.A.* **97**, 8087 (2000).
- A. Grinvald, L. Anglister, J. A. Freeman, R. Hildesheim, A. Manker, *Nature* **308**, 848 (1984).
- A. Sterkin et al., *Soc. Neurosci. Abstr.* **25**, 784 (1999).
- Supplementary Web material is available on Science Online at www.sciencemag.org/cgi/content/full/295/5554/512/DC1.
- D. Shoham et al., *Neuron* **24**, 791 (1999).
- S. Celebri, S. Thorpe, Y. Trotter, M. Imbert, *Vis. Neurosci.* **10**, 811 (1993).
- I. Shevelev, G. Sharaev, N. Lazareva, R. Novikova, A. Tikhomirov, *Neuroscience* **56**, 865 (1993).
- M. Volgushev, T. R. Vidyasagar, X. Pei, *Vis. Neurosci.* **12**, 621 (1995).
- All surgical and experimental procedures were in accordance with NIH guidelines. Twelve hemispheres from nine adult cats were used in this study. In three of these hemispheres, six different orientations were presented; in nine hemispheres, two orientations were presented. Cats were initially anesthetized intramuscularly with ketamine (15 mg kg⁻¹) and xylazine (1 mg kg⁻¹), supplemented with atropine (0.05 mg kg⁻¹). After tracheotomy, the animals were artificially respirated and anesthetized with 1 to 1.5% (0.6 to 1% during recording) halothane in a mixture of equal O₂ and N₂O. The skull was opened above area 18, and the dura was resected. During recording, paralysis was obtained with succinylcholine chloride (20 mg kg⁻¹ hour⁻¹, intravenously). The cats' eyes were fitted with zero-power contact lenses, and external lenses were used to focus the eyes on the screen. Additional details have been described previously (25). The exposed cortex was stained for 2.5 to 3 hours with the oxonol dye RH-1692 or RH-1691. A FUJIX HR Deltaron 1700 camera with an array of 128 by 128 detectors, each monitoring an area 64 mm by 64 mm, was used for data acquisition. The camera was connected to in-house software (DyeDAQ) and hardware. Details of the data acquisition setup and procedure are described in (79). Stimuli were full-screen 100% contrast black/white square-wave gratings of 0.2 cycles per degree drifting for 500 ms at 6 Hz. Between stimuli, the screen was blank with a luminance of 49 cd m⁻², equal to the mean luminance during stimulation. A recording epoch of 1 s surrounded each stimulus presentation. Fourteen stimuli were interleaved pseudorandomly. There were six orientations, starting from the horizontal and increasing in 30° increments, each in two drifting directions, and two blanks (gray screen). The stimuli were displayed binocularly with the VSG series 3 on a 38 cm by 29 cm, 640 pixel by 480 pixel monitor, located 50 cm from the cat's eyes, at a refresh rate of 150 Hz.
- For each orientation, we calculated the evoked response, which is a series of single-condition maps (25), corresponding to the series of acquired data frames. The recorded value at each pixel was first divided by the average value at that pixel before stimulus onset (to remove slow stimulus-independent fluctuations in illumination and background fluorescence levels), and this value was then divided by the value obtained for the blank condition. This procedure eliminates most of the noise due to heartbeat and respiration (76), and the result reflects neuronal activity after subtraction of spontaneous activity. To obtain the evoked response for each orientation, we averaged the responses to the two directions of motion. The data were then weakly band-pass filtered (250 to 2500 nm, 2D Butterworth filter); high-pass filtration was used to remove nonreproducible global differences in the responses to different orientations, whereas low-pass filtration was used to smooth the orientation maps (Fig. 2). Smoothed data were subsequently used. However, we verified that this smoothing did not affect the reported results.
- T. Bonhoeffer, A. Grinvald, *J. Neurosci.* **13**, 4157 (1993).
- N. V. Swindale, *Biol. Cybern.* **78**, 45 (1998).
- The Gaussian is not a cyclic function, in contrast to stimulus orientation. Therefore, for each pixel we assigned orientation 0 to the stimulus giving the strongest response (averaged over the duration of the response) and centered the other responses around it. The angle at which the Gaussian peaked was the preferred orientation, relative to the orientation around which the pixel's tuning curve was centered. In addition, centering each pixel's response enabled us to look at the tuning curve averaged over pixels, as shown in Figs. 1C and 3. A Gaussian with four parameters—width, amplitude, preferred orientation, and offset—was fitted to each tuning curve, with Matlab's nonlinear least-squares minimization function. The width parameter of the Gaussian was translated into HWHH (by multiplying by $\sqrt{2\ln 2}$). The amplitude parameter was taken to be the MD, and the offset is the NSC.
- The tuning curve is more selective when MD increases and the width and NSC decrease. Therefore we define selectivity index as MD/(HWHH × NSC), where NSC is the raw (unfiltered) evoked response measured at the orthogonal orientation (Fig. 1B, red).
- D. Y. Ts'o, R. D. Frostig, E. E. Lieke, A. Grinvald, *Science* **249**, 417 (1990).
- S. Chung, D. Ferster, *Neuron* **20**, 1177 (1998).
- J. S. Anderson, M. Carandini, D. Ferster, *J. Neurophysiol.* **84**, 909 (2000).
- M. Carandini, D. Ferster, *J. Neurosci.* **20**, 470 (2000).
- M. Volgushev, J. Pernberg, U. T. Eysel, *Eur. J. Neurosci.* **12**, 257 (2000).
- Sterkin et al., manuscript in preparation.
- To quantify the evoked DA notch, we defined a DA notch index (Fig. 4) as the absolute value of the second derivative, normalized to the first derivative, and summed over the two relevant frames (in which the deceleration and acceleration take place). This index agrees with qualitative assessment of notch size, as perceived by eye.
- At present we do not rule out the involvement of fast cortical processing, during the first 10 ms, in determining preferred orientation and tuning width because of current signal-to-noise limitations. Decreased sensitivity of optical imaging to events occurring in layer IV is another factor influencing its ability in detecting early events. However, the onset of the early optical signal coincides with the average earliest events detected by single-unit or intracellular recording [see, for example, (22)].
- D. J. Heeger, *Vis. Neurosci.* **9**, 181 (1992).
- L. J. Borg-Graham, C. Monier, Y. Fregnac, *Nature* **393**, 369 (1998).
- J. Anderson, D. Ferster personal communication.
- To obtain 99% confidence intervals for the fit parameters (Fig. 3, B and C), we performed a bootstrap procedure. One thousand data sets, equal in size to the real observed data set, were generated by drawing data points with replacements from the real data set. For each such synthetic data set, Gaussian fits were obtained (for each frame). The interval between 0.5 and 99.5% for each frame is shown (Fig. 3, B and C).
- We thank R. Hildesheim for synthesizing RH-1692 and RH-1691. We are grateful to D. Ferster, R. Shapley, and S. Barash, as well as to past and present members of our lab, including F. Chavane, D. Jancke, E. Seidemann, A. Shmuel, H. Slovin, and I. Vanzetta for critical comments on an earlier version of this manuscript. We thank D. Eitner, Y. Toledo, and C. Wijnbergen for technical assistance. Supported by grants from the Enoch, Goldsmith, and Glasberg Foundations.

3 September 2001; accepted 20 November 2001